Transactions of the Materials Research Society of Japan 27 [1] 287-290 (2002)

Heat Capacity Anomaly Due to the Ferroelectric Phase Transition in $Pb(Sc_{1/2}Ta_{1/2})O_3$

Yosuke Moriya, Hitoshi Kawaji, Takeo Tojo and Tooru Atake
Materials and Structures Laboratory, Tokyo Institute of Technology
Fax: 81-45-924-5339, e-mail: kawaji@thermo.rlem.titech.ac.jp

The heat capacity of the ferroelectric perovskite compound, $Pb(Sc_{1/2}Ta_{1/2})O_3$, was measured between 5 and 300 K by a relaxation method. A broad anomaly with two peaks at 283.1 K and 293.7 K was found in the heat capacity curve. The mechanism of the double peaks was discussed comparing with the data of dielectric constants, and a possibility of a new phase between the two peaks was pointed out. A broad heat capacity hump around 50 K implies high density of states of lattice vibrations in the low frequency region in $Pb(Sc_{1/2}Ta_{1/2})O_3$.

Key words: ferroelectric material, heat capacity, $Pb(Sc_{1/2}Ta_{1/2})O_3$, phase transition, relaxor

1. INTRODUCTION

The complex oxide of perovskite structure, $A(B'B'')O_3$, containing Pb as an A-site ion tends to be so-called relaxor. The relaxor ferroelectric compounds are characterized by large frequency-dependent dielectric constant extending in wide temperature range [1]. Since the broad peak in the dielectric constant seems to be caused by a phase transition, it has been called "diffused" phase transition [2]. However, no structural change has been observed in the X-ray and neutron diffraction measurements [3], and it is considered that no phase transition in the usual meaning occurs in the compound of relaxor ferroelectrics. On the other hand, the peak temperature at which the dielectric constant shows a maximum decreases with decreasing the attempt frequency [1]. Because of such relaxation phenomena, the relaxor is also considered as a kind of dipole glass and the glass-like properties have been studied extensively.

Lead magnesium niobate $Pb(Mg_{1/3}Nb_{2/3})O_3$ (PMN) is a typical perovskite relaxor of cubic structure *Pm*3*m* [4]. Two types of microstructures associated with the relaxor properties have been proposed for PMN. One is the chemically ordered domain of about 2 nm size, in which the two B-site ions is ordered in 1:1 ratio and a strong random electric field is induced locally [5]. The other is a rhombohedral ferroelectric region of about 10 nm size distributed in the cubic paraelectric matrix. The polarization of each rhombohedral ferroelectric region is randomly orientated to the eight [111] directions in the cubic matrix, and therefore the averaged structure of PMN is always of cubic symmetry [6]. It is considered that the rhombohedral ferroelectric region tends to grow as the temperature decreases but the random electric fields induced by the chemically ordered domains disturb the growth, and thus PMN does not undergo a ferroelectric phase transition without an external field [7].

On the other hand, it is known that the chemically ordered domain can grow in the whole crystal and the two B-site ions can be ordered in 1:1 ratio in $Pb(B'_{1/2}B''_{1/2})O_3$ type of the complex perovskite such as $Pb(Sc_{1/2}Ta_{1/2})O_3$ [8]. In this case, the ferroelectric phase transition occurs in the sample with highly ordered B-site cations [9,10]. The phase transition behavior has been known to be strongly influenced by the B-site ordering. The highly ordered sample shows the ferroelectric phase transition at about 290 K, and it becomes to exhibit so-called diffuse phase transition with increasing the disorder. Although the phase transition behavior has been studied attentively [11-16], the mechanism is still unclear. In the present study, we have carried out the heat capacity measurements for PST single crystal and discussed the mechanism of ferroelectric phase transition.

2. EXPERIMENTAL

The single crystal sample of PST was prepared by a flux method [17]. The powders of Sc_2O_3 (Rare Metallic Co., Ltd., 99.9 % purity), and Ta_2O_5 (Hikotaro Shudzui Co., Ltd., 99.9 % purity) were mixed in the equal molar ratio, and the mixture was heated in an electric furnace at 1300 °C for 24 h. The precursor, $ScTaO_4$, and PbO (Rare Metallic Co., Ltd., 99.99 % pure) were mixed with a small amount of excess PbO (about 3 mol%), and calcined at 800 °C for 2 h. The calcined powder was reground and then heated at 1300 °C for 1 h. X-ray diffraction analysis of the obtained powder confirmed the perovskite structure. The mixture of $PbO\text{-}PbF_2\text{-}B_2O_3$ was used as a flux in the mass ratio of PST: PbO: PbF_2: B_2O_3 = 0.15: 0.40: 0.40: 0.05. The mixture was put into a platinum crucible with a cover, and it was heated rapidly in a vertical tube furnace to 1250 °C. After holding the sample at 1250 °C for 4 h, it was cooled to 1000 °C at a rate of 3 $°Ch^{-1}$, and then to 900 °C at 5 $°Ch^{-1}$, and finally it was taken out to room temperature. The flux was dissolved with hot nitric acid, and the products were separated. As the crystal of PST is of simple cube, they could be easily separated by handwork from the others such as co-precipitated pyrochlore structure phases. The crystals were translucent with light brownish yellow, and the maximum grain size was about 3 mm. These crystals were identified with PST by powder X-ray diffraction. The order parameter of the B-site cation distribution was estimated as to be 0.80 using the powder X-ray diffraction data according to the method described in the previous report [10].

The heat capacity of the as grown PST single crystal was measured with a relaxation method between 2 and 300 K using PPMS (Quantum Design Inc.). The mass of the single crystal sample used was 25.41 mg.

The dielectric constant was also measured at 1 kHz for the same crystal as that used for calorimetry. The results were compared with those of the heat capacity measurements.

3. RESULTS AND DISCUSSION

The measured molar heat capacity of PST is shown in Fig. 1. A broad anomaly with two peaks at 283.1 K and 293.7 K is clearly seen in the heat capacity curve, and it should be attributed to the ferroelectric phase transition. The anomaly region is shown in an enlarged scale in Fig. 2 together with the heat capacity of PMN [18]. In Fig. 2, the normal heat capacity of PST due to the lattice vibrations is almost the same as that of PMN. Thus, the excess heat capacity due to the ferroelectric phase transition in PST can be estimated by subtracting the heat capacity of PMN. Small contribution of the tail of the heat capacity anomaly above 300 K was estimated by smooth extrapolation. The phase transition enthalpy and entropy obtained by integrating the excess heat capacity are 130 $Jmol^{-1}$ and 0.46 $JK^{-1}mol^{-1}$, respectively.

Although the phase transition has been reported as a single transition between cubic and ferroelectric rhombohedral structures, the heat capacity anomaly has two peaks at 283.1 K and 292.7 K as seen in Figs. 1 and 2. The dielectric constant (Fig. 3) measured at 1 kHz for the same crystal shows a peak at 293 K corresponding to the higher temperature peak of the heat capacity anomaly. However, below the peak, a small hump is at about 283 K on the shoulder, which corresponds to the lower temperature peak in the heat capacity curve. These results indicate that a new crystalline phase might be between the cubic and rhombohedral phases.

Debye temperatures of PST and PMN calculated from the molar heat capacities assuming $15N_A$ degrees of freedom are shown in Fig. 4, where N_A is Avogadro constant. The both curves are in good agreement with each other in the whole temperature range except for the phase transition region between 250 and 300

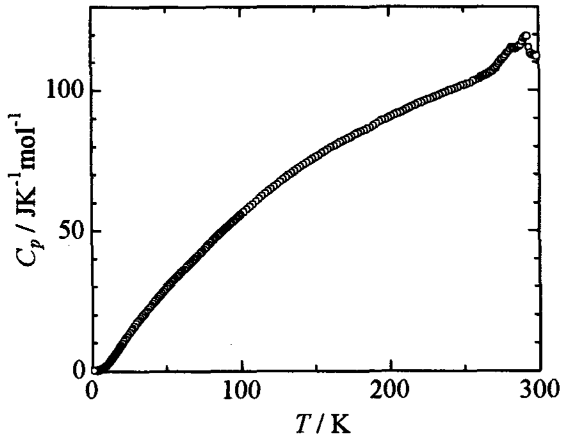

Fig. 1. Measured molar heat capacity of PST single crystal.

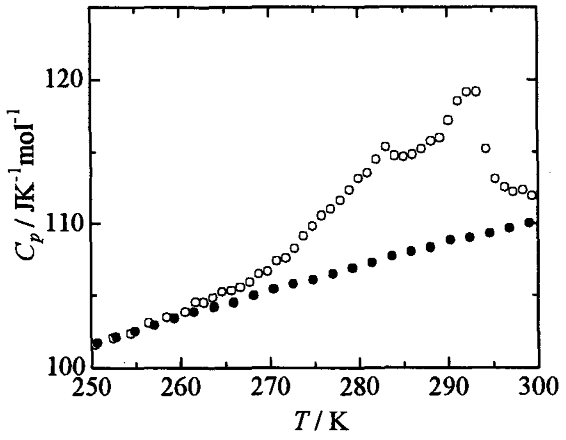

Fig. 2. Heat capacity of PST and PMN single crystals near the ferroelectric phase transition of PST.
○: PST, ●: PMN

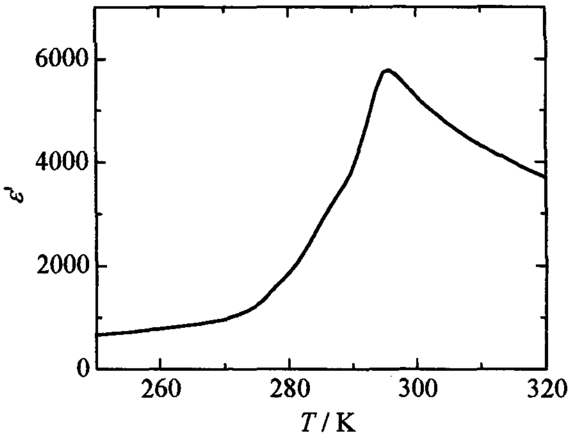

Fig. 3. Dielectric constant of PST single crystal near the ferroelectric phase transition temperature.

K, which means that the lattice vibrations are very similar to each other. The Debye temperatures of about 500 K around 200 K is very high comparing with KBr (ca. 180 K). Therefore the crystal of PST should be very hard. It is remarkable that the Debye temperature shows very steep curve of decreasing with decreasing temperature below 200 K, with a minimum of 180 K at about 10 K. Below 10 K, the curve goes up again, which is very common tendency in ordinary crystals. However, such a deep valley with depth of about 300 K indicates very large excess heat capacity over the normal lattice heat capacity in the low temperature region.

Such abnormal heat capacity curve can be seen rather clearly in the plots of C_pT^{-1} vs. T given in Fig. 5, in which very broad humps are at about 50 and 80 K. The higher temperature hump is observed commonly in typical perovskite crystals such as $BaTiO_3$ and $SrTiO_3$; at 130 and 100 K, respectively [19]. However, the lower temperature hump at about 50 K is observed only in PST and in PMN (at about 40 K) [18], and thus it might be a characteristic property of relaxors.

To investigate the abnormal heat capacity curve of PST described above, we analyzed the heat capacity using Debye and Einstein models, and box type of density of states for lattice vibrations. For the acoustic modes of $3N_A$ degrees of freedom, the Debye characteristic temperature was estimated as 230 K from the elastic constant of PMN reported by Tu et al. [20]. As PST has $15N_A$ degrees of freedom per mole of formula unit, the other contribution should be the optical modes of $12N_A$ ($15N_A$-$3N_A$) degrees of freedom. For these contributions, we assumed three non-dispersive modes (Einstein model) and two dispersive modes (box type of density of states). On the basis of these models, the fitting to the measured heat capacity was performed by a non linear least square method. The suitable initial values were used for both function's parameters (a characteristic temperature and degrees of freedom) and the each parameter was changed independently until calculated values converged to good fitting to the heat capacity data.

The results of the calculation by the non-linear least square method are shown in Figs. 5 and 6, and the numerical data are tabulated in Table 1. In Fig. 5, the calculated heat capacity denoted by a solid line shows very good agreement with the measured heat capacity data. Although the present model is extremely simple, the results of the calculation show fairly good agreement with those of the experiments, and some important characteristic properties can be pointed out for the crystal of PST. In Fig. 6, the lowest Einstein type mode at 55 K plays very much important role in the low temperature heat capacity hump at about 50 K mentioned above. It is worth noting that any models can never realize the low temperature heat capacity of PST

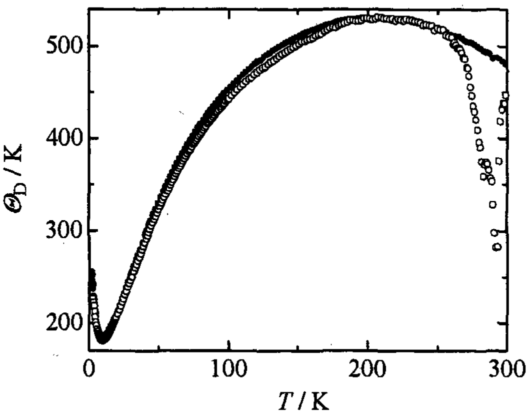

Fig. 4. Debye temperatures of PST and PMN single crystals calculated from the measured heat capacities assuming $15N_A$ degrees of freedom. ○: PST, ●: PMN.

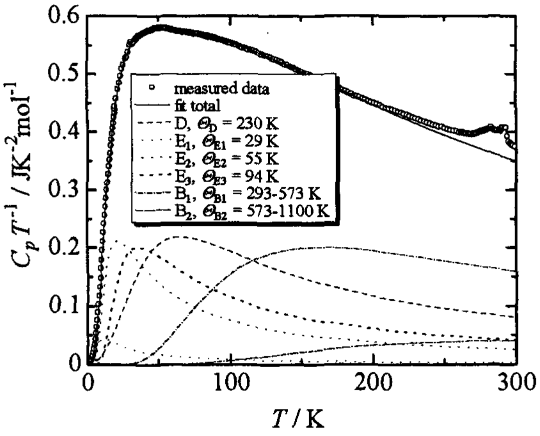

Fig. 5. Molar heat capacity of PST. The solid line is the result of the fitting, and the dashed line and others denote the individual contributions.

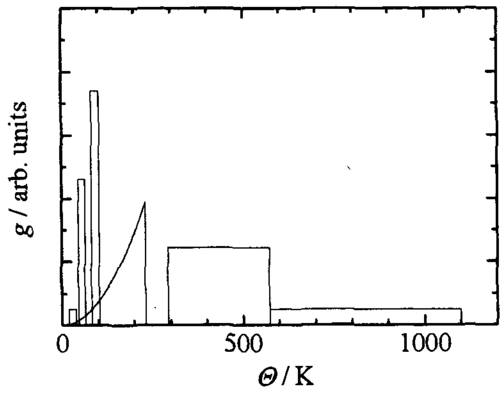

Fig. 6. Density of states of lattice vibrations in PST obtained by fitting to the measured heat capacity.

without this lowest energy mode. We have found similar results for PMN [18]. In PMN, however, the growth of the rhombohedral ferroelectric region is disturbed in the low temperature region, and no phase transition has been reported down to liquid helium temperature. Therefore it is considered that PMN is in very much constrained state at low temperatures, which should cause the low frequency modes in the lattice vibration. On the other hand, the ferroelectric phase transition occurs in PST. In the present study, however it has been found that PST also has similar low energy modes to those of PMN. Thus consequently it might be that the phase transition in PST is not completed, but some disorder may remain in B-site. Further studies are highly required to clarify this mechanism.

Table 1. Results of the fitting calculation by non-linear least square method. D: Debye model, E_1, E_2, E_3: Einstein model, B_1, B_2: box shaped type model.

model	Θ / K	*Degrees of Freedom* / N_A
D	230	3
E_1	29	0.1
E_2	55	0.9
E_3	94	1.5
B_1	293-573	6.8
B_2	573-1100	2.7

References
[1] D. Viehland, S.J. Jang, L.E. Cross and M. Wuttig, *Jpn. J. Appl. Phys*, **33**, 1969 (1994).
[2] G.A. Smolensky, V.A. Isupov, A.I. Agranovskaya and S.N. Popov, *Soviet Phys. –Solid State*, **2**, 2584 (1961).
[3] P. Bonneau, P. Garnier, G. Calvarine, E. Husson, J.R. Gavarri, A.W. Hewat and A. Morell, *J. Solid State Chem.*, 91, 350 (1991).
[4] P. Bonneau, P. Garnier, E. Husson and A. Morell, *Mat. Res. Bull.*, 24, 201 (1989).
[5] A.D. Hilton, D.J. Barber, C.A. Randall and T.R. Shrout, *J. Mater. Sci.*, 25, 3461 (1990).
[6] A.D. Hilton, C.A. Randall, D.J. Barber and T.R. Shrout, *Ferroelectrics*, 93, 379 (1989).
[7] V. Westphal, W. Kleeman and M.D. Glinchuk, *Phys. Rev. Lett.*, 68, 847 (1992).
[8] G.A. Smolenskii, *Soviet Phys. Solid State*, **1**, 150 (1959).
[9] C.G.F. Stenger, F.L. Scholten and A.J. Burggraaf, *Solid. State. Commun.*, **32**, 989 (1979).
[10] N. Setter and L.E. Cross, *J. Mater. Sci.*, **15**, 2478 (1980).
[11] N. Setter and L.E. Cross, *J. Appl. Phys.*, **51**, 4356 (1980).
[12] N. Setter and L.E. Cross, *Ferroelectrics*, **37**, 551 (1981).
[13] K.Z. Baba-kishi and D.J. Barber, *J. Appl. Cryst.*, **23**, 43 (1990).
[14] L.Y. Cai, X.W. Zhang and X.R. Wang, *Mater. Lett.*, **20**, 169 (1994).
[15] R. Blinc, A. Gregorovic, B. Zalar and R. Pirc, *Phys. Rev. B*, **61**, 253 (2000).
[16] S.N. Gvasaliya, S.G. Lushnikov, I.G. Siny, I.L. Sashin, T.A. Shaplygina and R. Blinc, *Physica B*, **276-278**, 485 (2000).
[17] N. Setter and L.E. Cross, *J. Cryst. Growth*, **50**, 555 (1980).
[18] S.N. Gvasaliya, S.G. Lushnikov, Y. Moriya, H. Kawaji and T. Atake, *Physica B*, **305**, 90 (2001).
[19] S.S. Todd and R.E. Lorenson, *J. Am. Chem. Soc.*, **74**, 1952 (1952)
[20] C.-S. Tu, V.H. Schmit and I.G. Siny, *J. Appl. Phys.*, **78**, 5665 (1995).

(Received December 21, 2001; Accepted January 31, 2002)